Electronic structures and magnetisms of the $Co_2TiSb_{1-x}Sn_x$ ($x = 0$, 0.25, 0.5) Heusler alloys: A theoretical study of the shape-memory behavior*

Wang Li-Ying(王立英)[a)b)], Dai Xue-Fang(代学芳)[b)], Wang Xiao-Tian(王啸天)[b)], Lin Ting-Ting(林婷婷)[a)], Chen Lei(陈 磊)[a)], Liu Ran(刘 然)[a)], Cui Yu-Ting(崔玉亭)[a)], and Liu Guo-Dong(刘国栋)[a)b)†]

[a)] *School of Physics and Electronic Engineering, Chongqing Normal University, Chongqing* 400044, *China*
[b)] *School of Materials Science and Engineering, Hebei University of Technology, Tianjin* 300130, *China*

(Received 5 May 2015; revised manuscript received 16 August 2015; published online 20 October 2015)

The total energy, electronic structures, and magnetisms of the $AlCu_2Mn$-type $Co_2TiSb_{1-x}Sn_x$ ($x = 0$, 0.25, 0.5) with the different lattice parameter ratios of c/a are studied by using the first-principles calculations. It is found that the phase transformation from the cubic to the tetragonal structure lowers the total energy, indicating that the martensitic phase is more stable and that a phase transition from austenite to martensite may happen at a lower temperature. Thus, a ferromagnetic shape memory effect can be expected to occur in these alloys. The $AlCu_2Mn$-type $Co_2TiSb_{1-x}Sn_x$ ($x = 0$, 0.25, 0.5) alloys are weak ferrimagnets in the austenitic phase and martensitic phase.

Keywords: Heusler alloy, martensitic transformation, ferromagnetic shape memory alloy

PACS: 62.20.fg, 63.20.dk, 31.10.+z **DOI:** 10.1088/1674-1056/24/12/126201

1. Introduction

The ferromagnetic shape memory effect was first discovered in Ni_2MnGa alloy in 1984.[1] At that time, the investigation on the related physical effect mainly focused on the large magnetic-field-induced strain.[1–3] Over the past 30 years, in succession, several material systems with Heusler structure, such as Ni–Fe–Ga,[4] Co–Ni–Ga(Al),[5–7] Mn–Ni–Ga(Al, In),[8–10] Ni–Mn–In (Sn or Sb),[11–13] and Mn_2PtIn,[14] have been found to be ferromagnetic shape memory alloys (FSMAs).[15–20] Accompanied by more and more FSMAs, more physical effects, such as magnetic-field-induced shape memory effect,[12] large magnetoresistance,[21,22] large magnetocaloric effect,[23] and exchange bias[24] were also developed in FSMAs. The various physical effects of FSMAs have received much attention and made them a promising candidate for the future technological applications in many fields. Therefore, efforts to explore new FSMAs and to improve their properties are in progress.

Co-based Heusler alloy is one of the important systems among the FSMAs family. The Co–Ni–Ga[5] and Co–Ni–Al[25] have been reported to be FSMAs. However, the relevant investigations on the ferromagnetic shape memory effect in CoTi-based alloys were rarely carried out. Up to now, although Co_2TiZ (Z = Al, Ga, Si, Ge, Sn, Sb)[26–28] have been investigated widely in theory and experiment, most of the investigations focus on their half-metallic properties. Especially, Co_2TiSb alloy is almost forgotten for it cannot crystallize into a pure $AlCu_2Mn$-type structure.[27] In this paper, we will focus on $Co_2TiSb_{1-x}Sn_x$ ($x = 0$, 0.25, 0.5) alloys. We will investigate the martensitic transformation and the magnetism in the alloys by using the first-principles calculations.

2. Computational methods

The electronic structures were calculated by using the pseudopotential method with a plane-wave basis set based on density-functional theory.[29,30] The interactions between the atomic core and the valence electrons are described by the ultrasoft pseudopotential.[31] The electronic exchange–correlation energy has been treated under the generalized gradient approximation (GGA). For all cases, a plane-wave basis set cut-off of 400 eV was used and 182 k points were employed in the irreducible Brillouin zone. The convergence tolerance in the calculations was selected to 1×10^{-6} eV/atom.

3. Results and discussion

3.1. Structure and geometry optimization

Heusler alloy with chemical composition X_2YZ, consists of four interleaving f.c.c. sublattices along a body diagonal with one formula unit per unit cell.[32] It contains $8X$ atoms, $4Y$ atoms, and $4Z$ atoms per unit cell. The $AlCu_2Mn$-type crystallizes into the $L2_1$ structure (space group $Fm\bar{3}m$) and

*Project supported by the Chongqing City Funds for Distinguished Young Scientists, China (Grant No. cstc2014jcyjjq50003), the Basic and Frontier Research Project of Chongqing City, China (Grant No. cstc2013jjB50001), the Project of Chongqing Normal University, China (Grant No. 13XLB030), and the Project of Scientific Research for High Level Talent in Colleges and Universities of Hebei Province, China (Grant No. GCC2014042).

†Corresponding author. E-mail: gdliu1978@126.com

© 2015 Chinese Physical Society and IOP Publishing Ltd

$CuHg_2Ti$-type (space group $F\bar{4}3m$) structures that are two different atom arrangement forms in Heusler alloys.[32] For $AlCu_2Mn$-type $Co_2TiSb_{1-x}Sn_x$ alloy, two Co atoms occupy 8*c* $(1/4,1/4,1/4)$ and $(3/4,3/4,3/4)$ Wyckoff positions and the Ti atom enters 4*a* $(0,0,0)$, leaving 4*b* $(1/2,1/2,1/2)$ to Sb and Sn atoms, and the structure model is shown in Fig. 1(a). For the $CuHg_2Ti$-type structure, two Co atoms occupy 4*a* $(0,0,0)$ and 4*c* $(1/4,1/4,1/4)$ Wyckoff positions, Ti and Sb or Sn atoms are located at 4*b* $(1/2,1/2,1/2)$ and 4*d* $(3/4,3/4,3/4)$ positions, respectively, as shown in Fig. 1(b). To determine the equilibrium lattice parameter and test the site preference in $Co_2TiSb_{1-x}Sn_x$ ($x = 0$, 0.25, 0.5), we perform the total energy (E_t) calculations on $Co_2TiSb_{1-x}Sn_x$ with the $AlCu_2Mn$-type and $CuHg_2Ti$-type structure in non-magnetic (NM) and ferromagnetic (FM) state, respectively.

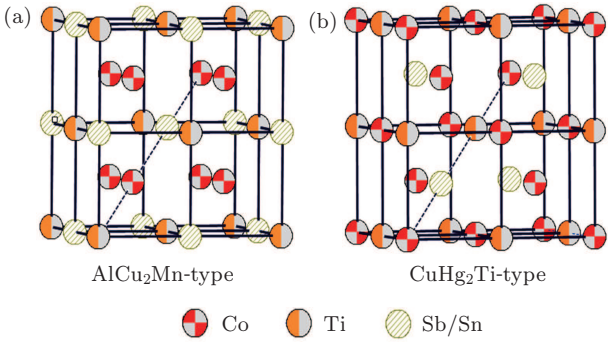


Fig. 1. (color online) Unit cell configurations for (a) $AlCu_2Mn$-type structure and (b) $CuHg_2Ti$-type structure $Co_2TiSb_{1-x}Sn_x$ ($x = 0$, 0.25, 0.5) alloys.

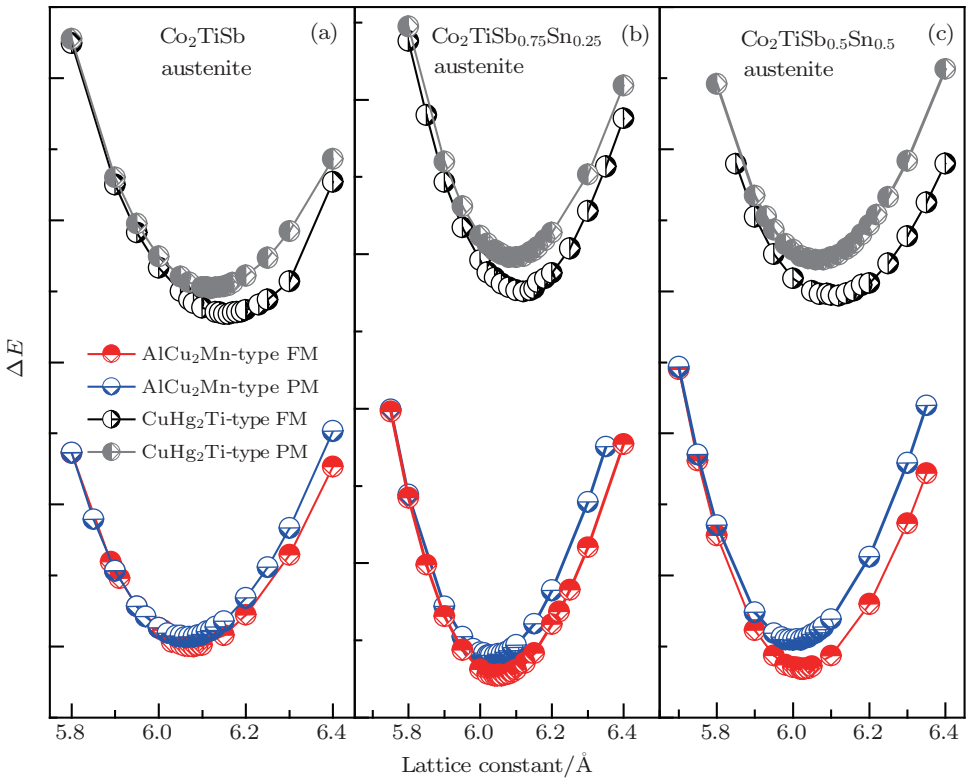


Fig. 2. (color online) Variations of total energy with lattice parameter for cubic $AlCu_2Mn$-type and $CuHg_2Ti$-type (a) Co_2TiSb, (b) $Co_2TiSb_{0.75}Sn_{0.25}$, and (c) $Co_2TiSb_{0.5}Sn_{0.5}$ in the non-magnetic (PM) and ferromagnetic (FM) states.

Table 1. Calculated structural, energy, and magnetic properties of Co_2TiSb, $Co_2TiSb_{0.75}Sn_{0.25}$, and $Co_2TiSb_{0.5}Sn_{0.5}$ alloys corresponding to the ground state. ΔE_t and ΔM are the energy difference and magnetic moment difference between the martensitic phase ($c/a > 1$) and the cubic phase ($c/a = 1$).

Alloys	Structure	a,b/Å	c/Å	c/a	M_{tot}/μ_B	M_{Co}/μ_B	M_{Ti}/μ_B	ΔE_t/(meV/f.u.)	$\Delta M/\mu_B$
Co_2TiSb	cubic	6.080	6.080	1	1.56	0.82	–0.14		
	tetragonal	5.787	6.713	1.16	1.23	0.72	–0.27	–108	–0.33
		6.207	5.834	0.94	1.34	0.74	–0.20		
$Co_2TiSb_{0.75}Sn_{0.25}$	cubic	6.04	6.04	1	1.68	0.82	–0.20		
	tetragonal	5.799	6.553	1.13	1.41	0.75	–0.28	–67	–0.27
		6.081	5.959	0.98	1.67	0.87	–0.20		
$Co_2TiSb_{0.5}Sn_{0.5}$	cubic	6.02	6.02	1	1.92	1.01	–0.26		
	tetragonal	5.832	6.415	1.10	1.65	0.85	–0.32	–14	–0.27

The curves of total energy versus the lattice parameters are shown in Fig. 2. It can be seen that the FM state is lower in the total energy for both $AlCu_2Mn$-type and $CuHg_2Ti$-type structures. The total energy of $AlCu_2Mn$-type structure is lower than that of $CuHg_2Ti$-type structure, which indicates that $Co_2TiSb_{1-x}Sn_x$ ($x = 0$, 0.25, 0.5) alloys prefer to crystallize into $AlCu_2Mn$-type structure. The atom arrangement forms in $Co_2TiSb_{1-x}Sn_x$ ($x = 0$, 0.25, 0.5) alloys are consistent with the site preference rule proposed in Ref. [24] where they showed that the site preference of 3d elements is determined by the number of the valence electrons and the elements with less d electrons prefer to occupy the B sites, whereas elements with more electrons prefer to occupy the (A, C) sites.[25] The achieved equilibrium lattice parameters are 6.08 Å, 6.04 Å, and 6.02 Å for $AlCu_2Mn$-type $Co_2TiSb_{1-x}Sn_x$ ($x = 0$, 0.25, 0.5). The data are also collected in Table 1.

3.2. Martensitic transformation in $Co_2TiSb_{1-x}Sn_x$ ($x = 0$, 0.25, 0.5) alloys

The first-principles calculations are used for analyzing and predicting the phase stability and potential martensitic transformations by calculating the total energy and electronic structures of the target system.[8,9,33–35] Next, the tetragonal distortion is investigated as the potential pathway to martensitic transformations. That is, we simulate the martensitic transformation by changing the axis ratio (c/a) from the cubic phase to the non-modulated tetragonal phase. In the calculations, the volume of the unit cell remains constant.

The E_t–c/a curves are shown in Fig. 3 for $AlCu_2Mn$-type $Co_2TiSb_{1-x}Sn_x$ alloys. From Fig. 3, it can be seen that the global minimum of the total energy is at $c/a = 1.16$ where the lattice parameters are $a = b = 5.787$ Å and $c = 6.539$ Å, and a local energy minimmum occurs at $c/a = 0.94$ for the Co_2TiSb alloy. The phenomenon of two minima of the total energy is also observed in the well-known FSMA Ni_2MnGa.[36] At a local energy minimum of $c/a = 0.94$, the system may undergo a shuffling transformation, and at a global energy minimum of $c/a = 1.16$, the tetragonal martensite is more stable for Co_2TiSb alloy. At $c/a = 1.16$, the driving force (the total energy difference between the tetragonal martensite phase and the cubic austenite phase) is as large as -108 meV/f.u. which is far higher than the previously reported driving forces, i.e., -7.08 meV for FSMAs Ni_2MnGa,[37] -30.10 meV for Ni_2FeGa,[37] and -9.29 meV for Mn_2NiGa.[38] Furthermore, the degree of distortion of $c/a = 1.16$ is smaller than those of Ni_2MnGa ($c/a = 1.22$),[37] Ni_2FeGa ($c/a = 1.33$)[37] and Mn_2NiGa ($c/a = 1.23$).[38] A smaller degree of distortion implies that the martensitic transformation in the system needs a smaller driving force. So the results indicate that the $AlCu_2Mn$-type Co_2TiSb alloy has a sufficient thermodynamic driving force to overcome the resistance of the phase transformation. That is, $AlCu_2Mn$-type Co_2TiSb alloy is a potential FSMA.

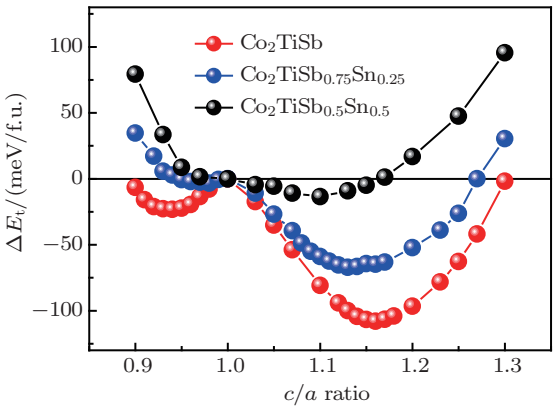


Fig. 3. (color online) Variations of total energy difference (ΔE_t) between cubic ($c/a = 1$) and tetragonally-distorted phase with c/a ratio in the constant volume for the $Co_2TiSb_{1-x}Sn_x$ ($x = 0$, 0.25, 0.5) alloys.

From Fig. 3, we can also see that the cases of alloys $Co_2TiSb_{0.75}Sn_{0.25}$ and $Co_2TiSb_{0.5}Sn_{0.5}$ are quite similar to a scenario of Co_2TiSb alloy in the shape of the E_t–c/a curve. Two minima of total energy are also observed for $Co_2TiSb_{0.75}Sn_{0.25}$ and $Co_2TiSb_{0.5}Sn_{0.5}$ alloys. The main difference is that the degrees of distortion at two minima of total energy and the driving force decrease with the increase of Sn content. The local minimum occurs at $c/a = 0.98$ and 1.0 for $Co_2TiSb_{0.75}Sn_{0.25}$ and $Co_2TiSb_{0.5}Sn_{0.5}$ alloys, respectively. Especially, we should notice that the local minimum occurs at $c/a = 1.0$ for $Co_2TiSb_{0.5}Sn_{0.5}$ alloys, which implies that the cubic structure (austenite) is at the local minimum and the shuffling transformation can be ruled out in this alloy. The global minima are at $c/a = 1.13$ and 1.10 respectively, and the driving forces are -67 meV/f.u. and -14 meV/f.u. for $Co_2TiSb_{0.75}Sn_{0.25}$ and $Co_2TiSb_{0.5}Sn_{0.5}$ alloys, respectively. Although the driving force decreases with the increase of Sn content, $Co_2TiSb_{0.75}Sn_{0.25}$ and $Co_2TiSb_{0.5}Sn_{0.5}$ alloys still have the driving forces about equal to or higher than those of FSMAs reported previously. In addition, the c/a values of 1.13 and 1.10 are also smaller. The energy differences between the cubic and the tetragonal phases are also listed in Table 1. All these results illustrated above indicate that $AlCu_2Mn$-type $Co_2TiSb_{1-x}Sn_x$ alloys are a series of new materials with martensitic transformation.

Figure 4(a) shows the density of state (DOS) patterns of the cubic $AlCu_2Mn$-type Co_2TiSb alloy. We mainly focus on the DOS near the Fermi level, for only the DOS is closely related to the structure stability. The Fermi level is located at a pseudogap in the spin-up channel. However, in the spin-down channel, the Fermi level is located at a high DOS peak, which indicates a high $N(E_f)$ (the density of states at the Fermi level). It has been reported that high $N(E_f)$ reduces the structure stability while low $N(E_f)$ has the opposite effect.[39,40] Figure 4(a) shows the total and partial DOS of the tetragonal

$AlCu_2Mn$-type Co_2TiSb. It is seen that the tetragonal distortion does not affect the general configuration of the total DOS. A main difference from the cubic $AlCu_2Mn$-type Co_2TiSb is that the sharp peak at the Fermi level in the spin-down channel is split into two relative weak peaks when the c/a ratio is 0.94. More obviously, the sharp peak is deeply split into two parts and a pseudogap occurs at the Fermi level at the $c/a = 1.16$. The occurrence of the pseudogap indicates that the hybridization between Co and Ti is strengthened. The strong d–d hybridization helps to stabilize the martensitic phase.[41] Similar results have been observed in Ni_2MnGa alloy and are known as the John–Teller effect, in which the density of state peak at the Fermi level in the cubic phase is divided into two peaks below and above the Fermi level with tetragonal distortion, resulting in a lower total energy and causing martensitic transformation.[42]

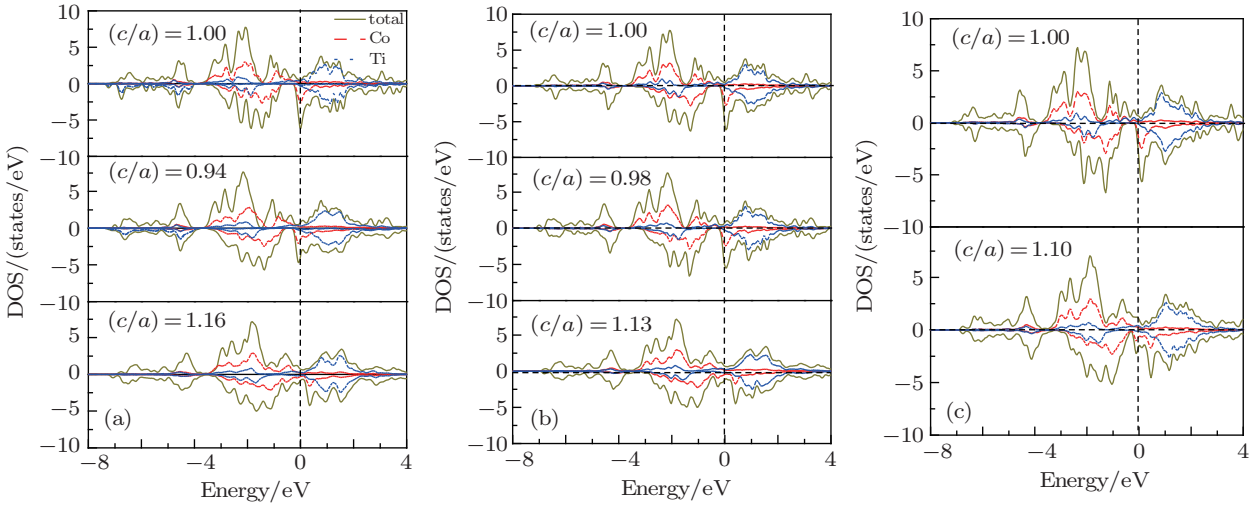


Fig. 4. (color online) Spin-polarized total and atom-projected densities of states for (a) Co_2TiSb, (b) $Co_2TiSb_{0.75}Sn_{0.25}$, and (c) $Co_2TiSb_{0.5}Sn_{0.5}$, calculated at the cubic phase, the local minimum of total energy and the global minimum of total energy. The Fermi energy is considered to be zero.

For the cubic and tetragonal $AlCu_2Mn$-type alloys $Co_2TiSb_{1-x}Sn_x$ ($x = 0.25$, 0.5), we show the DOS and the PDOS in Figs. 4(b) and 4(c). It is found that the Fermi level shifts to the low energy in both spin-up and spin-down channels when Sn is partly substituted for Sb in cubic $Co_2TiSb_{1-x}Sn_x$, which is obviously attributed to the less valence electrons of Sn atom than those of Sb atom to fill in the states. So, the Fermi level shifts from the high DOS peak toward a gap in the spin-down channel. The $N(E_f)$ decreases with increasing Sn content, which indicates that the doping Sn makes the cubic $AlCu_2Mn$-type structure more stable for the $Co_2TiSb_{1-x}Sn_x$ system. For the $Co_2TiSb_{1-x}Sn_x$ ($x = 0.25$, 0.5) alloys, the change of DOS induced by the transformation from cubic to tetragonal structure is similar to the undoped $AlCu_2Mn$-type Co_2TiSb alloy.

3.3. The magnetic properties of the $AlCu_2Mn$-type $Co_2TiSb_{1-x}Sn_x$ ($x = 0$, 0.25, 0.5) alloys

The total and atomic magnetic moments are indicated in Table 1 for the cubic and various tetragonal $Co_2TiSb_{1-x}Sn_x$ ($x = 0$, 0.25, 0.5) alloys. Generally, the Co atoms each have a large magnetic moment and are the main contributors to the magnetization for the $AlCu_2Mn$-type $Co_2TiSb_{1-x}Sn_x$ ($x = 0$, 0.25, 0.5) alloys. The Ti atoms each show a smaller and negative magnetic moment. So, the $AlCu_2Mn$-type $Co_2TiSb_{1-x}Sn_x$ ($x = 0$, 0.25, 0.5) alloys are weak ferrimagnets. From the DOS patterns of cubic $AlCu_2Mn$-type $Co_2TiSb_{1-x}Sn_x$ ($x = 0$, 0.25, 0.5) alloys ($c/a = 1$), it can be seen that the spin splitting has little change and it mainly is that the Fermi level equally shifts down in spin-up and spin-down channels to neutralize the decrease of the valence electrons caused by the doping Sn. Because the Fermi level is located in a pseudogap in the spin-up channel and a high peak in the spin-down channel, the states pushed above the Fermi level are more in the spin-down channel than in the spin-up channel when the Fermi level equally shifts down in two spin channels. So, the total and Co atomic magnetic moment increase with the increasing Sn content.

For the tetragonal $Co_2TiSb_{1-x}Sn_x$ ($x = 0$, 0.25) alloys at the local minimum, the total and atomic magnetic moments only have a small change with the Sn content due to the small degree of distortion. At the global minimum, the magnetization differences between the cubic and tetragonal structures are -0.33 μ_B, -0.27 μ_B, and -0.27 μ_B for $Co_2TiSb_{1-x}Sn_x$ ($x = 0$, 0.25, 0.5), respectively. A large magnetization difference between cubic and tetragonal structures implies a strong effect of the external magnetic field on the martensitic transformation from the cubic to tetragonal structure.

4. Conclusions

The electronic structure and magnetic properties of the Heusler alloys $Co_2TiSb_{1-x}Sn_x$ ($x = 0$, 0.25, 0.5) are studied

by the first-principles calculations. It is found that the cubic $AlCu_2Mn$-type $Co_2TiSb_{1-x}Sn_x$ alloys are unstable in total energy and electronic structure. It is possible that a martensitic transformation from cubic to tetragonal structure occurs in $AlCu_2Mn$-type $Co_2TiSb_{1-x}Sn_x$ alloys. The $Co_2TiSb_{1-x}Sn_x$ alloys are weak ferrimagnets. We predict that the $AlCu_2Mn$-type $Co_2TiSb_{1-x}Sn_x$ alloys are the new members of FSMAs' family.

References

[1] Webster P J, Ziebeck K R A, Town S L and Peak M S 1984 *Philos. Mag. B* **49** 295

[2] Ullakko K, Huang J K, Kantner C, O'Handley R C and Kokorin V V 1996 *Appl. Phys. Lett.* **69** 1966

[3] Wu G H, Yu C H, Meng L Q, Chen J L, Yang F M, Qi S R, Zhan W S, Wang Z, Zheng Y F and Zhao L C 1999 *Appl. Phys. Lett.* **75** 2990

[4] Liu Z H, Zhang M, Cui Y T, Zhou Y Q, Wang W H, Wu G H and Zhang X X 2003 *Appl. Phys. Lett.* **82** 424

[5] Wuttig M, Li J and Craciunescu C 2001 *Scr. Mater.* **44** 2393.

[6] Morito H, Fujita A, Kainuma R and Ishida K 2002 *Appl. Phys. Lett.* **81** 1657

[7] Karaca H E, Karaman I, Lagoudas D C, Maier H J and Chumlyakov Y I 2003 *Scr. Mater.* **49** 831

[8] Liu G D, Chen J L, Liu Z H, Dai X F, Wu G H, Zhang B and Zhang X X 2005 *Appl. Phys. Lett.* **87** 262504

[9] Sánchez Llamazares J L, Sanchez T, Santos J D, Pérez M J, Sanchez M L, Hernando B, Escoda L L, Suñol J J and Varga R 2008 *Appl. Phys. Lett.* **92** 012513

[10] Feng L, Ma L, Liu E K, Wu G H, Wang W H and Zhang W X 2012 *Appl. Phys. Lett.* **100** 152401

[11] Sutou Y, Imano Y, Koeda N, Omori T, Kainuma R, Ishid K and Oikawa K 2004 *Appl. Phys. Lett.* **85** 4358

[12] Kainuma R, Imano Y, Ito W, Sutou Y, Morito H, Okamoto S, Kitakami O, Oikawa K, Fujita A, Kanomata T and Ishida K 2006 *Nature* **439** 957

[13] Zhang Y Z, Cao J M, Tan C L, Cao Y J and Cai W 2014 *Chin. Phys. B* **23** 037504

[14] Luo H Z, Jia P Z, Liu G D, Meng F B, Liu H Y, Liu E K, Wang W H and Wu G H 2013 *Solid State Commun.* **170** 44

[15] Ullakko K, Huang J K, Kantner C, O'Handley R C and Kokorin V V 1996 *Appl. Phys. Lett.* **69** 1966

[16] James R D and Wuttig M 1998 *Phil. Mag. A* **77** 1273

[17] Wu G H, Yu C H, Meng L Q, Chen J L, Yang F M, Qi S R, Zhan W S, Wang Z, Zheng Y F and Zhao L C 1999 *Appl. Phys. Lett.* **75** 2990

[18] Fujita A, Fukamichi K, Gejima F, Kainuma R and Ishida K 2000 *Appl. Phys. Lett.* **77** 3054

[19] Oikawa K, Ota T, Ohmori T, Tanaka Y, Morito H, Fujita A, Kainuma R, Fukamichi K and Ishida K 2002 *Appl. Phys. Lett.* **81** 5201

[20] Kakeshita T, Takeuchi T, Fukuda T, Tsujiguchi M, Saburi T, Oshima R and Muto S 2000 *Appl. Phys. Lett.* **77** 1502

[21] Yu S Y, Liu Z H, Liu G D, Chen J L, Cao Z X, Wu G H, Zhang B and Zhang X X 2006 *Appl. Phys. Lett.* **89** 162503

[22] Barandiarán J M, Chernenko V A, Lázpita P, Gutiérrez J and Feuchtwanger J 2009 *Phys. Rev. B* **80** 104404

[23] Krenke T, Duman E, Acet M, Wassermann E F, Moya X, Manosa L and Planes A 2005 *Nat. Mater.* **4** 450

[24] Ma L, Wang W H, Lu J B, Li J Q, Zhen C M, Hou D L and Wu G H 2011 *Appl. Phys. Lett.* **99** 182507

[25] Oikawa K, Wulff L, Iijima T, Gejima F, Ohmori T, Fujita A, Fukamichi K, Kainuma R and Ishida K 2001 *Appl. Phys. Lett.* **79** 3290

[26] Webster P J and Ziebeck K R A 1973 *J. Phys. Chem. Solids* **34** 1647

[27] Lee S C, Lee T D, Blaha P and Schwarz K 2005 *J. Appl. Phys.* **97** 10C307

[28] Rai D P and Thapa R K 2013 *Chin. J. Phys.* **51** 812

[29] Payne M C, Teter M P, Allan D C, Arias T A and Joannopoulos J D 1992 *Rev. Mod. Phys.* **64** 1045

[30] Segall M D, Lindan P L D, Probert M J, Pickard C J, Hasnip P J, Clark S J and Payne M C 2002 *J. Phys.: Condens. Matter* **14** 2717

[31] Vanderbilt D 1990 *Phys. Rev. B* **41** 78

[32] Webster P 1969 *Contemp. Phys.* **10** 559

[33] Kandpal H C, Fecher G H and Felser C 2007 *J. Phys. D: Appl. Phys.* **40** 1507

[34] Liu G D, Dai X F, Yu S Y, Zhu Z Y, Chen J L, Wu G H, Zhu H and Xiao J Q 2006 *Phys. Rev. B* **74** 054435

[35] Luo H Z, Meng F B, Feng Z Q, Li Y X, Zhu W, Wu G H, Zhu X X, Jiang C B and Xu H B 2010 *J. Appl. Phys.* **107** 013905

[36] Entel P, Dannenberg A, Siewert M, Herper H C, Gruner M E, Comtesse D, Elmers H J and Kallmayer M 2012 *Metall. Mater. Trans. A* **43A** 2891

[37] Sahariah M B, Ghosh S, Singh C S, Gowtham S and Pandey R 2013 *J. Phys.: Condens. Matter* **25** 025502

[38] Felser C, Alijani V, Winterlik J, Chadov S and Nayak A K 2013 *IEEE Trans. Magn.* **49** 682

[39] Xu J H, Oguchi T and Freeman A J 1987 *Phys. Rev. B* **36** 4186

[40] Tobola J and Pierre J 2000 *J. Alloys Compd.* **296** 243

[41] Ye M, Kimura A, Miura Y, Shirai M, Cui Y T, Shimada K, Namatame H, Taniguchi M, Ueda S, Kobayashi K, Kainuma R, Shishido T, Fukushima K and Kanomata T 2010 *Phys. Rev. Lett.* **104** 176401

[42] Fujii S, Ishida S and Asano S 1989 *J. Phys. Soc. Jpn.* **58** 3657